Diagnostic value of abnormal chromosome 3p genes in small-cell lung cancer

CHUNXU MA[1*], JIHUA ZHAO[1*], YING WU[1], JUN WANG[2] and HAO WANG[1,3]

[1]Department of Nuclear Medicine, The First Affiliated Hospital of Kunming Medical University, Kunming, Yunnan 650000; [2]College of Physical Education, Yunnan Agricultural University, Kunming, Yunnan 650201; [3]Department of Nuclear Medicine, Sichuan Academy of Medical Sciences and Sichuan Provincial People's Hospital, School of Medicine, UESTC, Chengdu, Sichuan 610072, P.R. China

Received February 9, 2022; Accepted April 20, 2022

DOI: 10.3892/ol.2022.13330

Abstract. The diagnosis of small cell lung carcinoma (SCLC) remains a great challenge. Changes in chromosome 3p (chr3) genes are usually observed in the pathogenesis of lung cancer, which suggests that these chr3 genes may be a diagnostic marker in the early stage of SCLC. The present study explored the diagnostic value of the chr3 gene in SCLC using Bioinformatics. Furthermore, reverse transcription-quantitative PCR (RT-qPCR) was used to reveal the expression patterns of diagnostic biomarkers in human pulmonary alveolar epithelial cells and in the SCLC cell line NCI-H146. A total of 33 differentially expressed (DE) chr3 genes and 1,156 module genes associated with clinical features of patients with SCLC were identified and functional enrichment analysis indicated that all these genes were significantly enriched in cell cycle terms. The area under the receiver operating characteristic curve demonstrated that the overlapping genes of the DE-chr3 and module genes, namely cell division cycle 25 A (CDC25A), FYVE and coiled-coil domain autophagy adaptor 1 (FYCO1) and lipid raft linker 1 (RFTN1), were relatively accurate in distinguishing normal from SCLC samples, and may thus be considered diagnostic biomarkers. CDC25A was overexpressed in SCLC samples, while FYCO1 and RFTN1 were highly expressed in normal samples, as evidenced by the RT-qPCR results. Single-gene gene set enrichment analysis suggested that the diagnostic biomarkers were significantly associated with cell cycle, ATP-binding cassette transporter, immune cell differentiation, immune response and multiple respiratory disease pathways. Furthermore, a total of 141 drugs were predicted by The Comparative Toxicogenomics Database to be able to modulate the expression of the diagnostic biomarkers, of which 8 drugs were shared among the three aforementioned diagnostic biomarkers. The present study identified three novel and powerful diagnostic biomarkers for SCLC based on chr3 genes. Suggestions for the development and selection of drugs for clinical treatment based on diagnostic biomarkers were also provided.

Correspondence to: Dr Hao Wang, Department of Nuclear Medicine, The First Affiliated Hospital of Kunming Medical University, 295 Xichang Road, Kunming, Yunnan 650000, P.R. China
E-mail: 18810566155@163.com

Dr Jun Wang, College of Physical Education, Yunnan Agricultural University, 452 Fengyuan Road, Kunming, Yunnan 650201, P.R. China
E-mail: 158291721@qq.com

*Contributed equally

Abbreviations: SCLC, small-cell lung cancer; OS, overall survival; NSE, neuron-specific enolase; ProGRP, progastrin-releasing peptide; chr3, chromosome 3p; GEO, Gene Expression Omnibus; GSEA, Gene Set Enrichment Analysis; DEGs, Differential expression genes; WGCNA, weighted gene co-expression network analysis; UCSC, University of California Santa Cruz; GO, Gene Ontology; KEGG, Kyoto Encyclopedia of Genes and Genomes; IPKB, Ingenuity Knowledge Base; ROC, receiver operating characteristic; AUC, area under curve; HPAEpiC, human pulmonary alveolar epithelial cells; ATCC, American Type Culture Collection; RT-qPCR, reverse transcription-quantitative PCR

Key words: diagnosis, small-cell lung cancer, chromosome 3p gene, reverse transcription-quantitative PCR, drug prediction

Introduction

Lung cancer accounts for >10% of all cancer cases worldwide and is one of the most common types of cancer (1). In 2018, 781,000 newly confirmed cases of lung cancer and 626,000 mortalities were reported in China (2). Small cell lung carcinoma (SCLC), which is characterized by an unusually high proliferation rate, a strong propensity for early metastasis and poor prognosis, accounts for ~15% of all lung cancer cases. The 5-year survival rate of patients with SCLC after diagnosis is only 2.8%, with a median overall survival (OS) of ~10 months (3). In addition, the majority of patients have metastatic disease at diagnosis, with only 1/3 of them having earlier-stage disease, which increases the difficulty of clinical treatment (4). Therefore, early diagnosis of SCLC is of great importance to improve the OS of patients with SCLC.

At present, early detection of the majority of tumor types, including SCLC, mainly depends on the combination of patients' timely medical consultation, as well as imaging and other examinations. However, due to a variety of factors, including patients' delayed medical treatment and doctors' clinical experience, numerous patients are diagnosed at an advanced tumor stage. Conventional methods, such as image-guided percutaneous transthoracic puncture biopsy and bronchoscopy, are able to accurately detect various pathological tumor types and have a role in the diagnosis of tumors. However, biopsy and bronchoscopy are not appropriate for patients with respiratory inadequateness or unclear location of the tumor. With the continuous development of molecular biology, serum tumor markers, such as neuron-specific enolase (NSE) and progastrin-releasing peptide (ProGRP), have gradually become diagnostic markers for malignant tumors, including SCLC (5). However, their specificity is not always satisfactory due to the elevated NSE and ProGRP concentration in numerous patients. In addition, the concentration of NSE in hemolytic samples is also increased (6). Thus, identifying more reliable diagnostic markers to compensate for the deficiencies of these traditional serum markers is urgently required.

Chromosomal copy number variation is a hallmark of cancer (7). Loss of heterozygosity involving several chromosome 3p (chr3) regions accompanied by chr3 deletions is detected in almost 100% of SCLC cases. In addition, these changes appear early in the pathogenesis of lung cancer. Such 3p genetic alterations suggest that the short arm of human chr3 contains several tumor suppressor genes (8). Deletions in chr3 have been identified in lung adenocarcinoma tumors via the tumor sequencing project initiative (9). Chr3 common eliminated region 1 (C3CER1) on chr3p21.3 is a putative tumor suppressor region. C3CER1 loss of heterozygosity exceeds 90% in lung tumors compared with that of the putative tumor suppressor gene fragile histidine triad diadenosine triphosphatase (65%) and the tumor suppressor gene Von Hippel-Lindau (72%) (10). It is known that genetic and epigenetic abnormalities of several genes residing in the chr3 region are important for the development of SCLC, but it remains elusive how many they are and which of the numerous candidate tumor suppressor genes are key factors in SCLC pathogenesis. Therefore, exploring the diagnostic value of the chr3 gene in SCLC may facilitate the clinical diagnosis and prognosis of SCLC.

In the present study, gene expression data obtained from Gene Expression Omnibus (GEO) database were integrated to perform data mining and analysis of SCLC. Next, a series of co-differentially expressed genes were screened in SCLC. Several analyses were carried out based on these genes, including functional enrichment analysis, single-gene Gene Set Enrichment Analysis (GSEA) and drug identification. Furthermore, the mRNA levels of three diagnostic genes were detected in the SCLC cell line NCI-H146 by reverse transcription-quantitative PCR (RT-qPCR). The association between the genes in chr3 deletion regions and disease progression of SCLC was analyzed and therapeutic drugs were predicted based on these genes.

Materials and methods

Data source. The GSE40275 and GSE60052 datasets used in the present study were downloaded from the GEO database. The GSE40275 dataset (https://www.ncbi.nlm.nih.gov/geo/query/acc.cgi?acc=GSE40275) contained 43 normal lung tissue samples (from 14 normal cases) and 21 SCLC tissue samples (from 8 cases of SCLC) (Table SI). The mean age of the eight patients with SCLC (7 males and 1 female) in the GSE40275 dataset was 67.1 years (range 54-70 years). A total of 86 samples were included in the GSE60052 dataset (https://www.ncbi.nlm.nih.gov/geo/query/acc.cgi?acc=GSE60052), comprising 7 normal lung tissue (from 7 normal cases) and 79 tumor samples from patients with SCLC (Table SII). The GSE40275 dataset was primarily used for screening of differentially expressed genes (DEGs), weighted gene co-expression network analysis (WGCNA), diagnostic biomarker assessment and single-sample GSEA, while the GSE60052 dataset was employed for screening of DEGs and diagnostic biomarker assessment.

The 505 chr3 genes (Table SIII) were obtained from the Human Dec. 2013 (GRCh38/hg38) Assembly in the University of California Santa Cruz (UCSC) Genome Browser Database (https://genome.ucsc.edu).

Analysis of DEGs. DEGs were identified in the GSE40275 and GSE60052 datasets individually using the 'limma' package in R software. Genes that satisfied |log2 fold change (FC)|>1 and P<0.05 between normal and SCLC samples were considered as DEGs. The overlapping genes of DEGs (co-DEGs) in the above two datasets were obtained by Venn diagram analysis, which was performed on the jvenn online website (http://jvenn.tou-louse.inra.fr/app/example.html). DE-chr3 genes (overlapping genes between co-DEGs and chr3 genes) were also identified. Furthermore, visualization and embellishment of the Venn diagrams were achieved using the jvenn online website.

Metascape analysis. Metascape (http://metascape.org/) is a powerful tool for functional annotation analysis of genes (11) and was used in the present study to perform a comprehensive functional enrichment analysis of the DE-chr3 genes, including Gene Ontology (GO), Kyoto Encyclopedia of Genes and Genomes (KEGG) and Reactome analyses. GO analysis was performed in three categories: Cellular component (CC), molecular function and biological process (BP) (12). KEGG (13) and Reactome (14) analyses were used to explore the pathways in which genes may be involved. Terms with P<0.01 were considered to be significantly enriched.

Ingenuity pathway analysis (IPA). IPA (version 1-19; Qiagen Digital Insights) is a cloud-based, graphical bioinformatics software that mines genomic data for hidden biological significance from a biological pathway perspective. The Ingenuity Knowledge Base (IPKB), the core component of IPA, is a specialized biological interaction and functional annotation database that contains information on interactions between proteins, genes, compounds, cells, tissues, drugs and diseases. In the present study, the DE-chr3 genes were uploaded to IPKB and subjected to its Disease & Function analysis.

WGCNA. Genes with mean expression values (fragments per kilobase of exon per million mapped fragments) >1 were extracted from all SCLC samples (GSE40275 dataset)

Table I. Primer sequences for quantitative PCR.

Gene	Forward primer (5'-3')	Reverse primer (5'-3')
CDC25A	TATGAGCAACCACTGGAGGT	GTGACTGGGGTGTAAAAAGA
FYCO1	GTGGGGCAGGATTCGGAAAT	TGGGGATCAGGCTGTAGGTG
RFTN1	TTCCTCCTTAGACCACCCGA	AGTTCTCCACCATCTCCCTC
GAPDH	CGCTGAGTACGTCGTGGAGTC	GCTGATGATCTTGAGGCTGTTGTC

CDC25A, cell division cycle 25 A; FYCO1, FYVE and coiled-coil domain autophagy adaptor 1; RFTN1, lipid raft linker 1.

to perform WGCNA using clinical and expression data from the GSE40275 dataset. Clinical trait-related modules were constructed and module genes were identified in the R package WGCNA. In brief, a hierarchical clustering analysis was performed on the GSE40275 dataset samples to exclude outliers (i.e., the GSM990246 sample was an outlier and was excluded; Fig. S1A). The soft-threshold power was set to 11 (scale-free R^2=0.85). Modules were segmented by the dynamic tree-cutting algorithm and MEDissThres (the dissimilarity threshold of module eigengenes) was set to 0.5 to merge similar modules (Fig. S1B-D). Finally, Pearson correlations between module genes and clinical features were calculated. The genes in the modules that were most correlated with clinical features were considered to be module genes. It should be noted that, since the M-stage information for patients in the GSE40275 dataset was recorded as MX for all, the M-stage was not considered. Therefore, clinical characteristics included pathological T and N stages (pT, pN), tumor stage (stage), sex and age. Detailed functional annotation of module genes was performed by GO and KEGG enrichment analysis in the clusterProfiler package in R.

Receiver operating characteristic (ROC) curves and area under the curve (AUC) estimation based on diagnostic biomarkers. The overlapping genes of the module genes and DE-chr3 genes were obtained by Venn diagram analysis and subsequently used as candidate biomarkers. Next, ROC curves and their corresponding AUCs were established from the GSE40275 and GSE60052 datasets to evaluate the ability of candidate biomarkers to correctly diagnose disease. Only candidate biomarkers with an AUC >0.85 in both datasets were identified as diagnostic biomarkers for SCLC. Furthermore, expression profiles were extracted from the GSE40275 and GSE60052 databases to demonstrate the expression patterns of the selected biomarkers.

Cell culture. Human pulmonary alveolar epithelial cells (HPAEpiC) and the SCLC cell line NCI-H146 were purchased from the American Type Culture Collection. HPAEpiC cells were maintained in DMEM (HyClone; Cytiva) supplemented with 10% fetal bovine serum (FBS; Gibco; Thermo Fisher Scientific, Inc.) and 1% penicillin-streptomycin (Lonza Group, Ltd.). NCI-H146 cells were cultured in RPMI-1640 medium (MilliporeSigma) supplemented with 10% FBS and 1% penicillin-streptomycin. The cells were grown at 37˚C in a humidified atmosphere of 95% air and 5% CO_2. The experiments were carried out on cells of passage 10-25.

RNA extraction and RT-qPCR. Total RNA was extracted from HPAEpiC and NCI-H146 cells using TRIzol® reagent (Invitrogen; Thermo Fisher Scientific, Inc.). The concentration and quality of RNA were determined by spectrophotometry (Jinghua Technology) at 260 and 280 nm. Total RNA was reverse transcribed using the SureScript™ First-Strand cDNA Synthesis Kit (Genecopoeia, Inc.) according to the manufacturer's protocol. RT-qPCR was performed using the CFX96™ Real-Time PCR Detection System (Bio-Rad Laboratories, Inc.) using the BlazeTaq™ SYBR®-Green qPCR Mix 2.0 kit (Genecopoeia, Inc.) according to the manufacturer's instructions. The thermocycling conditions were as follows: Initial denaturation at 95˚C for 30 sec, followed by 40 cycles that each involved incubation at 95˚C for 10 sec, 60˚C for 20 sec and 72˚C for 30 sec. Relative expression values were calculated using the $2^{-\Delta\Delta Cq}$ method (15). The primers were synthesized by TsingKe Biological Technology and their sequences are listed in Table I.

Single-gene GSEA. Single-gene GSEA (in the R package clusterProfiler) was applied to analyze the pathways enriched by each diagnostic biomarker. In brief, samples were divided into high- and low-expression groups using the median expression of each diagnostic biomarker in the GSE40275 dataset. Subsequently, log2 FC values were calculated for all genes between the high- and low-expression groups for each diagnostic biomarker (of note, the DEGs between the high- and low-expression groups were not defined; only the difference between the two groups was analyzed) and were ranked from highest to lowest according to the log2 FC value. The sorted genes were used as the set of genes to be evaluated; simultaneously, the KEGG pathway was used as a pre-defined set of genes. Finally, single-gene GSEA was performed separately for each diagnostic biomarker in the clusterProfiler package to detect the enrichment of the pre-defined gene set in the set of genes to be evaluated. An adjusted P<0.05 for the pathway was considered to indicate a statistically significant difference.

Drug identification by the comparative toxicogenomics database (CTD). The CTD (http://ctdbase.org/) is a scientific database for describing associations between chemicals, genes and human diseases. For a certain gene, the CTD may provide the corresponding target compounds in a descending order of their interactions. In the present study, CTDs with default parameters were used to predict the candidate drugs for the selected biomarkers.

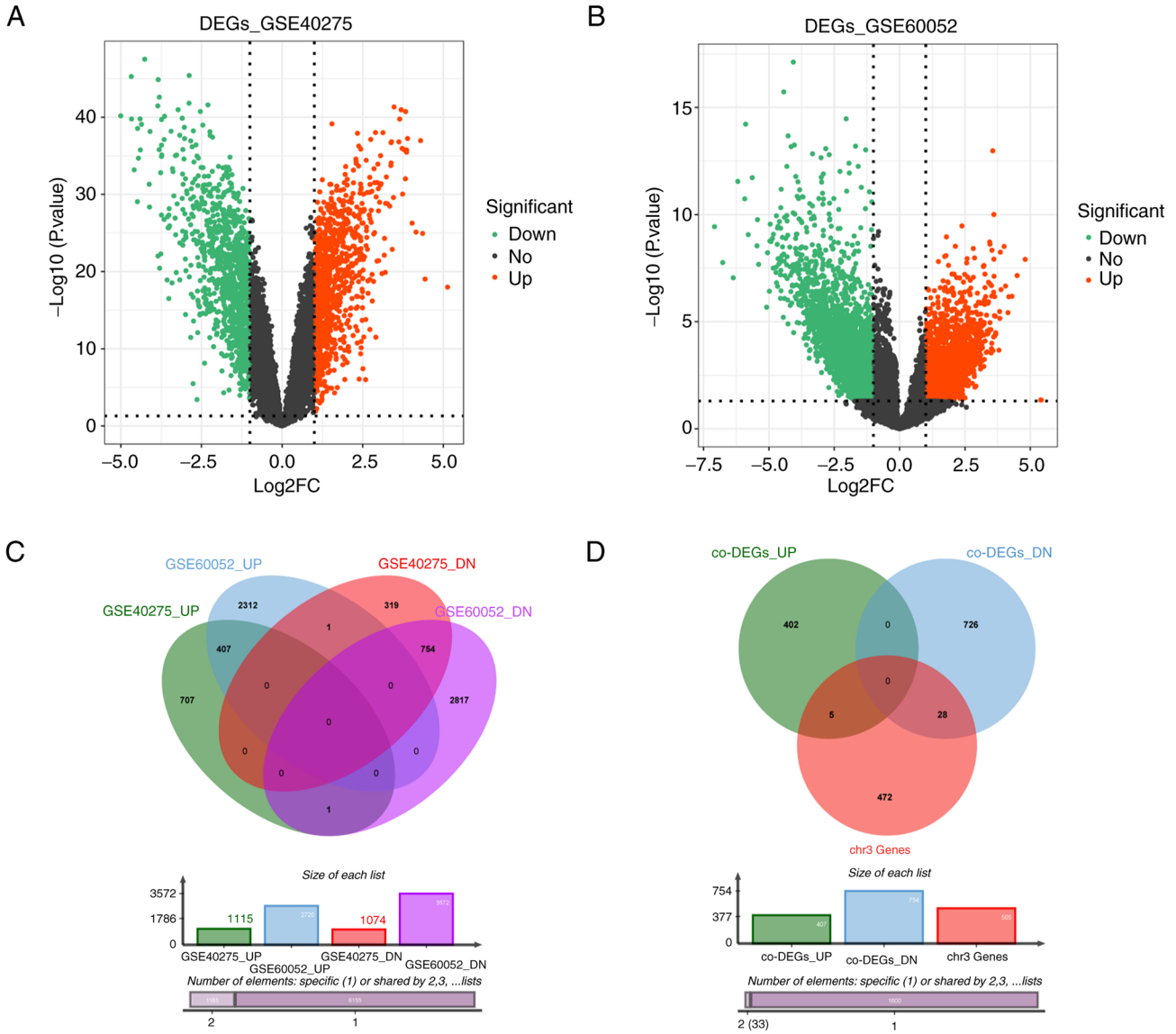

Figure 1. Identification of DEGs in SCLC. Volcano plots displaying the DEGs between SCLC and normal samples in the (A) GSE40275 and (B) GSE60052 datasets. (C) Co-DEGs of the two datasets. (D) Intersection between co-DEGs of the above two datasets and chr3 genes. DEGs, differentially expressed genes; SCLC, small cell lung carcinoma; FC, fold change; down/DN, downregulated; up, upregulated; no, not significantly changed; chr3, chromosome 3p.

Statistical analysis. Bioinformatics analysis was performed in R software. The complete drug-diagnostic biomarker network was visualized with Cytoscape software (v3.6.1; https://www.nigms.nih.gov/). For shared drugs, intersection analysis was performed on the jvenn online website. Subsequent shared drug-diagnostic biomarker networks were represented in the diagrams.net online network (https://app.diagrams.net/). Histograms were constructed using GraphPad Prism 8 software (GraphPad Software, Inc.) to indicate the association between the tissue type (normal and SCLC) and the mRNA levels of diagnostic biomarkers. Unless otherwise stated, $P<0.05$ was considered to indicate a statistically significant difference.

Results

Identification of the DE-chr3 genes associated with SCLC. In the GSE40275 dataset, a total of 2,189 DEGs between 21 SCLC and normal samples were identified, of which 1,115 were upregulated and 1,074 were downregulated (Fig. 1A; Table SIV). In total, 6,290 DEGs were extracted from the GSE60052 dataset (79 SCLC vs. 7 normal), including 2,720 upregulated and 3,572 downregulated genes (Fig. 1B; Table SV). Venn diagram analysis indicated that a total of 1,162 co-DEGs (407 upregulated and 755 downregulated genes) were differentially expressed between SCLC and normal samples in the above datasets (Fig. 1C; Table SVI). Subsequently, 505 genes located in chr3:1-90000000 were obtained by Human Dec. 2013 (GRCh38/hg38) assembly in the UCSC Genome Browser Database and were designated as chr3 genes (Table SIII). Fig. 1D revealed that only 33 of these 505 chr3 genes were co-DEGs, of which, 5 were upregulated and 28 were downregulated (Fig. S2A and B; Table SVII).

Based on Metascape-GO analysis, the DE-chr3 genes were observed to be closely associated with oxygen metabolic process, cell motility and regulation of inflammatory responses.

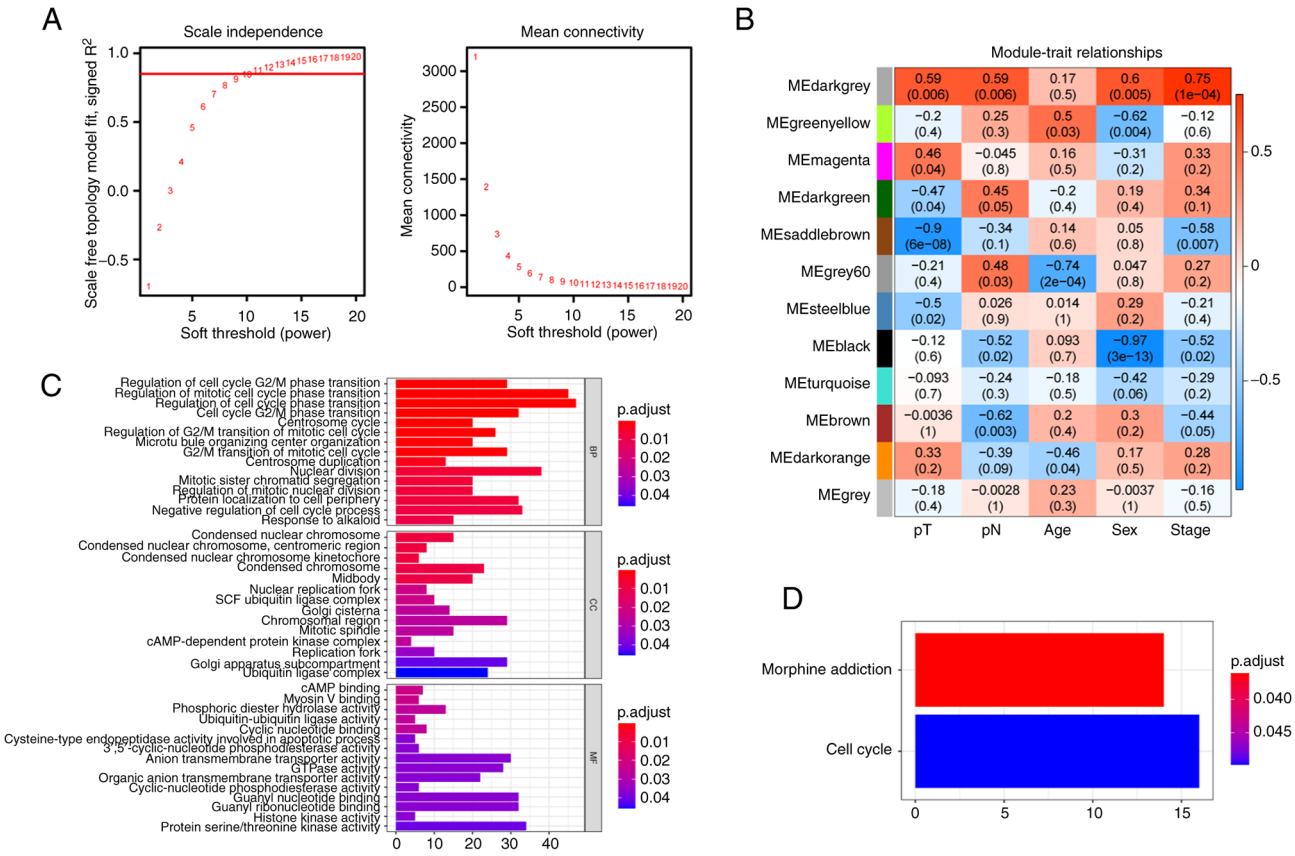

Figure 2. Identification of module genes and their functional annotation. (A) Soft threshold of scale independence and mean connectivity by weighted gene co-expression network analysis. (B) Associations between 12 co-expressed modules and clinical characteristics. (C) GO-biological process, GO-cellular component and GO molecular function analyses revealed that the aforementioned module genes were significantly enriched in various cell cycle-related terms. (D) Kyoto Encyclopedia of Genes and Genomes pathway analysis indicated that the cell cycle pathway was significantly enriched. GO, Gene Ontology; ME, module eigengene.

Unexpectedly, regulation of supramolecular fiber organization and supramolecular fiber organization were indicated to be significantly enriched (Fig. S2C-F; Table SVIII). Several supercoiled supramolecular polymeric fibers of self-sorted donor-acceptor molecules (supramolecular fibers) have been reported as markers of lung cancer (16). IPA's Disease & Function analysis revealed that these DE-chr3 genes were involved not only in cellular, tissue and organ development, but also in cancer, tumor morphology and respiratory diseases (Table SIX) which suggested that the DE-chr3 genes probably have an essential role in the development and progression of SCLC.

Search of module genes associated with clinical features of SCLC by WGCNA. WGCNA was performed on 20 SCLC samples from the GSE40275 dataset. With a soft threshold set to 11 (R^2=0.85), the gene network infinitely approximated the scale-free distribution (Fig. 2A). A total of 12 co-expressed modules were then identified (Fig. 2B). Correlations between modules and clinical characteristics were calculated, including age, sex, pT, pN and stage. The dark grey module was strongly associated with pT (r=0.59, P=0.006), pN (r=0.59, P=0.006), sex (r=0.6, P=0.005) and stage (r=0.75, P=1x10^{-4}). The dark grey module was selected as the hub module and 1,156 genes (Table SX) of this module were investigated in the subsequent analyses.

The potential functions of these module genes were also explored. GO-BP analysis revealed that these genes were significantly enriched in various cell cycle-related terms (Fig. 2C; Table SXI). Similarly, the KEGG pathway analysis also demonstrated that the cell cycle pathway was significantly enriched (Fig. 2D; Table SXII). These results suggested that the variation in cell cycle processes may be associated with SCLC progression.

Identification and assessment of diagnostic biomarkers for SCLC. To further identify biomarkers for SCLC, three overlapping genes for the DE-chr3 genes and the module genes were obtained, namely cell division cycle 25 A (CDC25A), FYVE and coiled-coil domain autophagy adaptor 1 (FYCO1) and lipid raft linker 1 (RFTN1) (Fig. 3A). The ability of the three overlapping genes to discriminate between normal and SCLC samples was subsequently assessed by ROC curves (Fig. 3B and C). CD25A had an AUC of 0.988 in the GSE40275 dataset and of 0.880 in the GSE60052 dataset; FYCO1 had AUCs of 1 and 0.944 in the GSE40275 and GSE60052 datasets, respectively; and RFTN1 had AUCs of 0.993 and 0.868 in the above GSE40275 and GSE60052 datasets, respectively. This suggested that the above three overlapping genes possessed a robust capacity to differentiate between the SCLC and normal groups and were therefore considered as diagnostic biomarkers for SCLC in subsequent analyses. CDC25A was upregulated in SCLC,

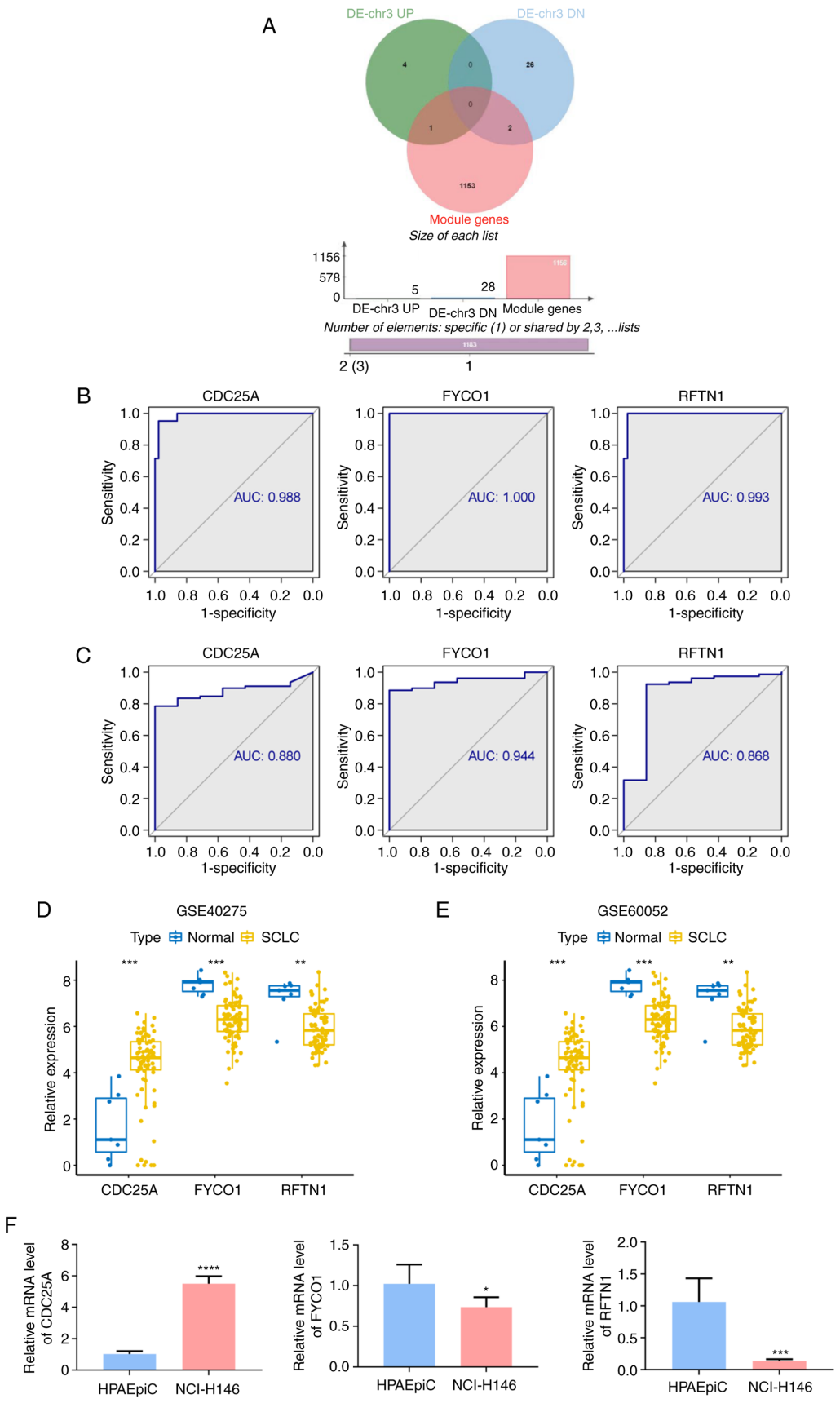

Figure 3. Identification of the three overlapping genes for the DE-chr3 and module genes in SCLC. (A) Venn diagram displaying the three overlapping genes for the DE-chr3 and module genes. The ability of the three overlapping genes to discriminate between normal and SCLC samples in the (B) GSE40275 and (C) GSE60052 datasets was assessed by receiver operating characteristic curves. Expression patterns of these three overlapping genes in the (D) GSE40275 and (E) GSE60052 datasets. (F) Reverse transcription-quantitative PCR results provided the relative mRNA levels of these three overlapping genes between NCI-H146 and human pulmonary alveolar epithelial cells. *P<0.05; **P<0.01; ***P<0.001; ****P<0.0001. DE, differentially expressed; chr3, chromosome 3p; SCLC, small cell lung carcinoma; DN, downregulated; UP, upregulated; AUC, area under the curve; CDC25A, cell division cycle 25 A; FYCO1, FYVE and coiled-coil domain autophagy adaptor 1; RFTN1, lipid raft linker 1.

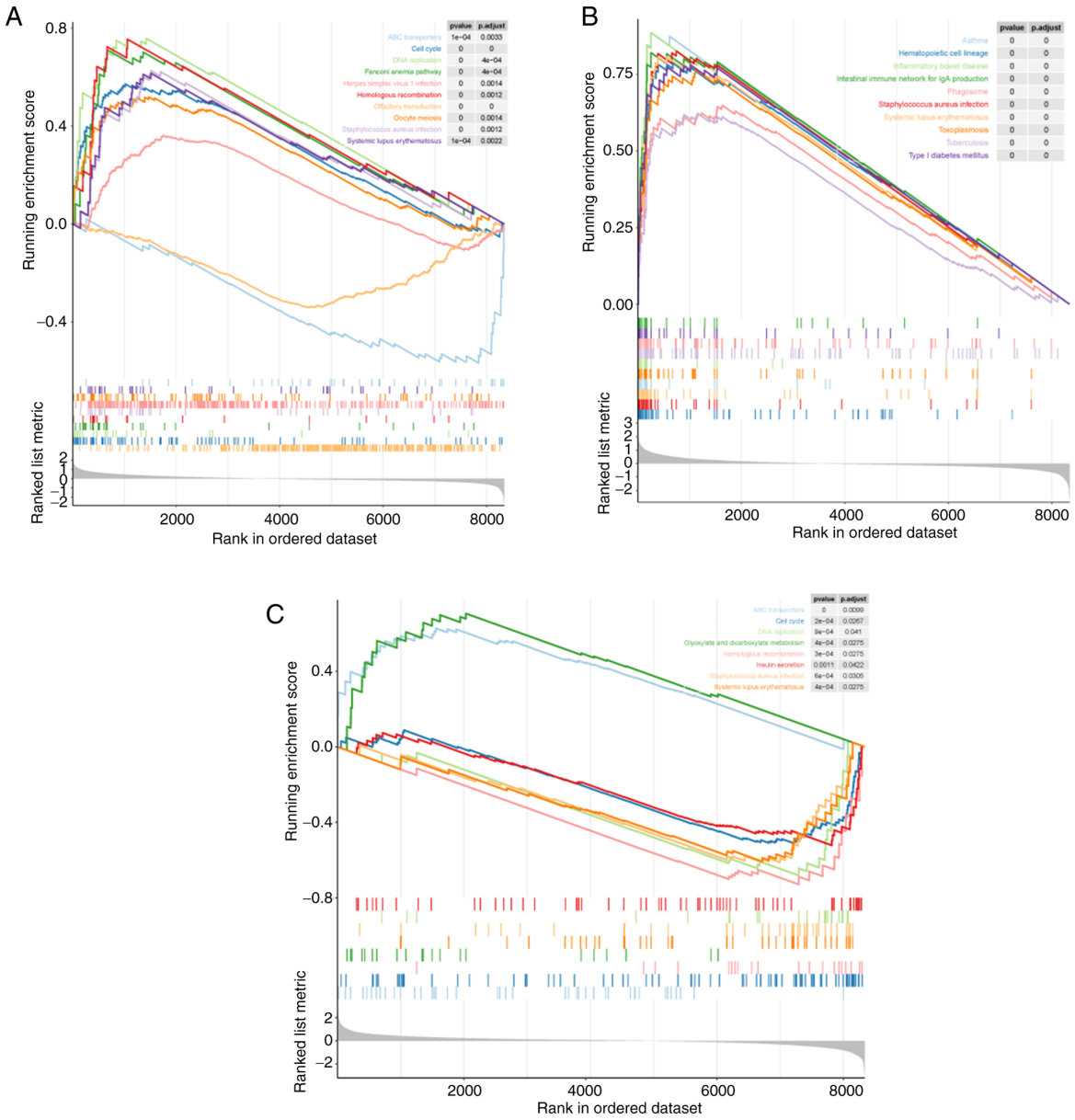

Figure 4. Functional annotation of each diagnostic biomarker. (A) Single-gene GSEA revealed that cell division cycle 25 A was enriched in 22 KEGG pathways. (B) Single-gene GSEA revealed that lipid raft linker 1 was significantly associated with 52 KEGG pathways. (C) Single-gene GSEA revealed that FYVE and coiled-coil domain autophagy adaptor 1 was mainly involved in 8 KEGG pathways. A merged enrichment plot from single-gene GSEA including enrichment score and gene sets is presented. GSEA, Gene Set Enrichment Analysis; KEGG, Kyoto Encyclopedia of Genes and Genomes.

whereas FYCO1 and RFTN1 were overexpressed in normal samples and the expression patterns of these genes were consistent between the GSE40275 (Fig. 3D) and GSE60052 (Fig. 3E) datasets. Consistently, the RT-qPCR results (Fig. 3F) revealed that CDC25A exhibited a higher expression level in NCI-H146 cells compared with that in HPAEpiC cells (P<0.0001), whereas FYCO1 and RFTN1 were significantly decreased in NCI-H146 cells (P=0.0421 and P=0.0005, respectively).

In addition, the association between the expression of diagnostic biomarkers and the clinical characteristics of SCLC were examined in the GSE40275 dataset. The results indicated that the three genes were significantly associated with pT, stage and sex. Specifically, CDC25A was markedly upregulated in pT4, stage IIIB and male patients (Fig. S3A); RFTN1 was markedly upregulated in pT4, stage III and male patients (Fig. S3B); and FYCO1 was upregulated in pT2, stage I and female patients, as well as those with pN0 (Fig. S3C).

Pathway enrichment analysis of each diagnostic biomarker. To reveal the potential pathways the diagnostic biomarkers are involved in, single-gene GSEA was performed for each diagnostic biomarker in the GSE40275 dataset. The results revealed that CDC25A was enriched in a total of 22 KEGG pathways (Fig. 4A; Table SXIII); RFTN1 was significantly associated with 52 KEGG pathways (Fig. 4B; Table SXIV); and FYCO1 was mainly involved in 8 KEGG pathways (Fig. 4C; Table SXV).

Specifically, all three diagnostic biomarkers were involved in the KEGG pathways of 'cell cycle', 'DNA replication' and 'homologous recombination'. This suggested that the diagnostic biomarkers may also be involved in the proliferation

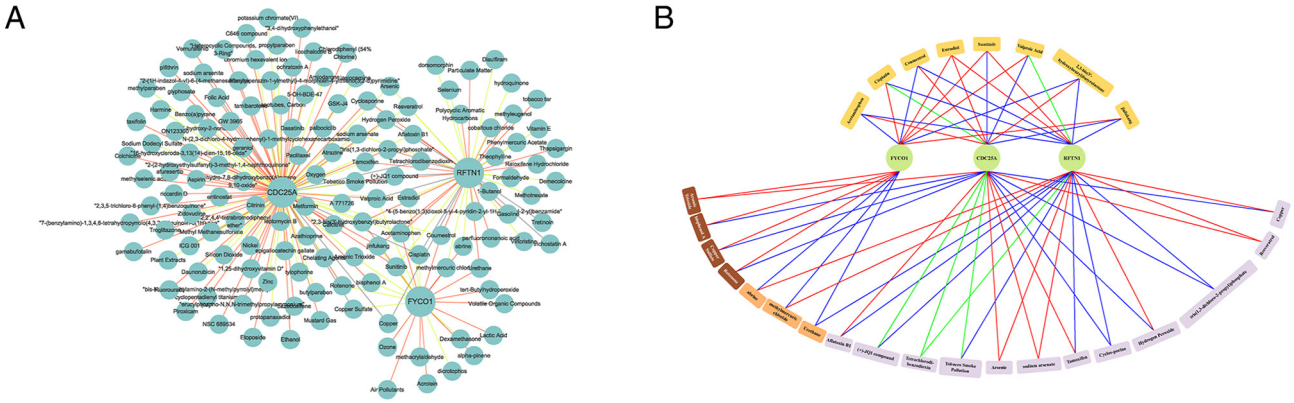

Figure 5. Pharmaceutical prediction for regulating the expression of diagnostic biomarkers by the Comparative Toxicogenomics Database. (A) A complete drug-diagnostic biomarker network was constructed using Cytoscape. The smaller circles represent the predicted drugs, while the larger circles are diagnostic biomarkers. The red, green and grey lines indicate upregulation, downregulation and both up- and downregulation, respectively. (B) Regulatory associations of 27 shared drugs (drugs shared by two diagnostic biomarkers and drugs shared by all three diagnostic biomarkers) with diagnostic biomarkers. Circles represent diagnostic biomarkers; rounded rectangles indicate predicted drugs (brown for drugs shared by CDC25A and FYCO1; orange for drugs shared by FYCO1 and RFTN1; purple for drugs shared by CDC25A and RFTN1; and yellow for drugs shared by all three diagnostic biomarkers); blue straight lines represent downregulation, red straight lines represent upregulation and green straight lines represent both up- and downregulation. CDC25A, cell division cycle 25 A; FYCO1, FYVE and coiled-coil domain autophagy adaptor 1; RFTN1, lipid raft linker 1.

process of tumor cells. Of note, the ATP-binding cassette '(ABC) transporter' pathway was significantly enriched by CDC25A and FYCO1. The ABC transporter superfamily is known to be a family of membrane transporter proteins. Increased intracellular drug pumping is considered one of the mechanisms of tumor multidrug resistance and numerous members of the ABC superfamily have also been indicated to be involved in tumor multidrug resistance (17-19). It was also observed that the 'drug metabolism-other enzymes' pathway was markedly associated with RFTN1. Such evidence indicated that diagnostic biomarkers may aid the development of novel drugs for SCLC. Of note, it was also observed that immune cell [T helper '(Th)17 cell differentiation', 'Th1 and Th2 cell differentiation', 'natural killer cell-mediated cytotoxicity', 'neutrophil extracellular trap formation'] and immune response ('antigen processing and presentation', 'cell adhesion molecules', 'chemokine signaling pathway', 'Fc e RI signaling pathway' and 'Rap1 signaling pathway')-related pathways were associated with RFTN1. The reason why SCLC is reportedly not sensitive to immunotherapy is the absence of a surface protein that triggers the immune response, and this innate deficiency may also be associated with tumor immune escape in SCLC (20). Therefore, it was hypothesized that RFTN1 may provide a theoretical basis and direction for identifying effective immunotherapeutic targets and mechanisms for SCLC. In addition, several respiratory diseases were also highlighted, including 'asthma' (CDC25A and RFTN1), 'tuberculosis' (RFTN1), 'influenza A' (RFTN1), 'coronavirus disease-COVID-19' (RFTN1) and 'pertussis' (RFTN1).

Pharmaceutical prediction for regulating the expression of diagnostic biomarkers. Based on the aforementioned results, CTD (21) was employed to predict potential pharmaceutical agents that may modulate the expression of diagnostic biomarkers. A total of 141 potential drugs were identified by CTD (Table SXVI). A complete drug-diagnostic biomarker network was constructed using Cytoscape, which contained 144 nodes with 223 edges (Fig. 5A). The regulatory associations of 27 shared drugs (drugs shared by two diagnostic biomarkers and drugs shared by all three diagnostic biomarkers) with diagnostic biomarkers are presented in Fig. 5B. Acetaminophen, cisplatin, coumestrol, estradiol, sunitinib, valproic acid, 2,3-bis(3'-hydroxybenzyl) butyrolactone and Jinfukang were the shared drugs for the three diagnostic biomarkers, which have potential to guide the development of novel drugs for SCLC (Table II).

Discussion

SCLC is the most aggressive form of lung cancer. Compared with NSCLC, SCLC is characterized by a rapid doubling time and early, widespread metastases. The lack of early detection modalities is one of the important barriers to progress in the diagnosis and treatment of SCLC. Therefore, novel biomarkers with high efficiency, sensitivity and specificity are urgently required for the diagnosis and prognosis of SCLC. Previous studies have indicated that chr3 alterations may be associated with the pathogenesis of SCLC (8). Thus, chr3 genes may become diagnostic biomarkers of SCLC.

The development of high-throughput sequencing has facilitated the search for genes and mechanisms potentially involved in cancer. Bioinformatics use genetic information to improve molecular diagnoses and drug therapies (22). Integrated bioinformatics analysis for the identification of therapeutic targets of certain cancers based on transcriptomics, proteomics and high-throughput sequencing may help to obtain novel information and to understand the potential underlying molecular mechanisms. In the present study, 33 DE-chr3 genes were identified, which may have an essential role in the development and progression of SCLC, and it was confirmed that the variation in cell cycle processes may be associated with SCLC progression according to GO-BP analysis. In addition, three overlapping genes were obtained for the DE-chr3 and the module genes (namely CDC25A, FYCO1 and RFTN1) by bioinformatics functional assessment.

Table II. The 8 shared predicted drugs for three diagnostic biomarkers and their interactions.

A, CDC25A∩FYCO1

	Interactions		
Predicted drug	CDC25A	FYCO1	RFTN1
Arsenic trioxide	UP	UP	N/A
Bisphenol A	DN	UP	N/A
Copper sulfate	DN	UP	N/A
Rotenone	DN	UP	N/A

B, CDC25A∩RFTN1

	Interactions		
Predicted drug	CDC25A	FYCO1	RFTN1
Aflatoxin B1	UP	N/A	DN
(+)-JQ1 compound	UP/DN	N/A	DN
Tetrachlorodi-benzodioxin	UP/DN	N/A	UP/DN
Tobacco smoke pollution	UP/DN	N/A	DN
Arsenic	UP	N/A	UP
Sodium arsenate	UP	N/A	UP
Tamoxifen	UP	N/A	DN
Cyclosporine	DN	N/A	DN
Hydrogen peroxide	DN	N/A	UP
Tris(1,3-dichloro-2-propyl)phosphate	DN	N/A	DN
Resveratrol	UP	N/A	UP
Copper	DN	N/A	UP

C, FYCO1∩RFTN1

	Interactions		
Predicted drug	CDC25A	FYCO1	RFTN1
Abrine	N/A	DN	UP
Methylmercuric chloride	N/A	DN	UP
Urethane	N/A	DN	DN

D, CDC25A∩FYCO1∩RFTN1

	Interactions		
Predicted drug	CDC25A	FYCO1	RFTN1
Acetaminophen	UP	DN	DN
Cisplatin	UP/DN	UP	DN
Coumestrol	UP	DN	DN
Estradiol	UP	UP	UP

Table II. Continued.

D, CDC25A∩FYCO1∩RFTN1

	Interactions		
Predicted drug	CDC25A	FYCO1	RFTN1
Sunitinib	DN	UP	UP
Valproic acid	DN	UP	UP/DN
2,3-bis (3'-hydroxybenzyl) butyrolactone	UP	DN	DN
Jinfukang	DN	UP	DN

CDC25A, cell division cycle 25 A; FYCO1, FYVE and coiled-coil domain autophagy adaptor 1; RFTN1, lipid raft linker 1; DN, down-regulated; UP, upregulated; N/A, not applicable.

CDC25A is one of the cell cycle regulation-related genes. CDC25A is mainly localized in the nucleus and controls G_1/S progression by dephosphorylation-dependent inactivation of cyclin E/cyclin-dependent kinase (CDK)2 and cyclin D/CDK4-6; G_2 phase progression by dephosphorylation of CDK1 and activation of the cyclin B1/CDK1 complex is a limiting step (23). A previous study suggested that CDC25A controls cell proliferation and tumorigenesis by changing the expression of proteins involved in cyclin D1 regulation and G_1/S transition (24). Maintenance of adequate CDC25A levels is important for genomic stability and tumor suppression (25). The activity and abundance of CDC25A are intricately regulated and CDC25A is frequently overexpressed in several cancer types (26-29). Butz *et al* (30) revealed that overexpression of CDK1 and CDC25A may have an important role in promoting pituitary tumors in the G_2/M transition phase. The present study suggested that the expression of CDC25A in SCLC was significantly increased and it was speculated that high expression of CDC25A in SCLC may also promote the occurrence and development of SCLC during the G_2/M transition phase. However, the specific mechanism requires to be further explored. Rao *et al* (31) observed that aberrant expression of the cell cycle regulation-related genes cyclin D1, cyclin E, cyclin A, CDC25A and CDK4 may facilitate the transcription and expression of genes associated with cell cycle progression. A previous study suggested that the cell cycle could be the pathway most closely associated with the pathogenesis of SCLC (22). However, the functions of the cell cycle and its regulatory proteins in SCLC have not been fully clarified thus far.

FYCO1 is a late Rab7 effector of autophagy that is required for the maturation of autophagosomes (32). FYCO1 has been reported to link autophagosomes to the microtubule plus-end movement motor kinesin, which promotes the maturation of autophagosomes and the formation of autophagolysosomes (32). Dionne *et al* (33) noticed that FYCO1 regulated the accumulation of post-mitotic midbodies by mediating light chain 3-dependent midbody degradation and FYCO1 was reported as one of the key genes involved in adenoma-to-carcinoma

transition in colorectal cancer (34). Another study indicated that the expression levels of FYCO1 in paired bladder tissue and urine samples were significantly lower in bladder cancer than in those in the control group (35). RFTN1 has been studied in numerous diseases. Wang *et al* (36) concluded that RFTN1 may be involved in the pathogenesis of glaucoma. Another study suggested that RFTN1 may participate in smoking behavior through modulating immune responses or interactions with glucocorticoid receptor α and androgen receptor (37). Zhao *et al* (38) explored molecular subtypes and core genes for lung adenocarcinoma and screened out two core genes: Contactin 4 (CNTN4) and RFTN1. The authors concluded that low expression of CNTN4 and RFTN1 predicted unfavorable clinical outcomes in patients with lung adenocarcinoma. The aforementioned studies demonstrated that FYCO1 and RFTN1 were involved in the occurrence and development of a variety of tumors and other diseases. However, the specific roles of CNTN4 and RFTN1 in the pathogenesis of SCLC have not been elucidated to date.

In the present study, it was determined that CDC25A was upregulated in SCLC samples, while FYCO1 and RFTN1 were upregulated in normal vs. SCLC samples. In addition, the three genes were significantly associated with pT, stage and sex of patients with SCLC. These results indicated that these three overlapping genes may have an important role in the development of SCLC. The results of single-gene GSEA for each diagnostic biomarker revealed potential pathways the diagnostic biomarkers are involved in, including 'proliferation process of tumor cells', 'immune cells' and 'immune response'. The specific roles of different diagnostic biomarkers in different pathways require to be further explored. The present results may facilitate the identification of novel targeted drugs to improve the therapeutic effect and prolong the survival time of patients with SCLC.

In the present study, pharmaceutical prediction for regulating the expression of diagnostic biomarkers was performed based on CTD. The results revealed that acetaminophen, cisplatin, coumestrol, estradiol, sunitinib, valproic acid, 2,3-bis(3'-hydroxybenzyl) butyrolactone and Jinfukang were the shared drugs for the aforementioned three diagnostic biomarkers, which may potentially aid the development of novel drugs for SCLC. A number of these drugs have been studied on lung cancer previously. A large cohort study indicated that total non-steroidal anti-inflammatory drug (NSAID) use was associated with a reduced risk of lung cancer, which suggested that NSAIDs may be useful for chemoprevention (39). Cisplatin, a well-known chemotherapeutic drug, has been used for the treatment of numerous human cancer types, including bladder, head and neck, lung, ovarian and testicular cancer (40). Cisplatin exerts its anticancer activity via multiple mechanisms, but the most accepted mechanism involves the generation of DNA lesions by interacting with purine bases on DNA, followed by the activation of several signal transduction pathways, which finally lead to apoptosis (41). Coumestrol is a natural compound exhibiting broad anticancer effects against skin melanoma, lung cancer and colon cancer cell growth. The anticancer effect of coumestrol is due to the direct targeting of haspin kinase (42). Que *et al* (43) confirmed that Jingfukang induces anticancer activity through oxidative stress-mediated DNA damage in circulating human lung cancer cells. Platta *et al* (44) observed that the histone deacetylase inhibitor valproic acid activates Notch1 signaling in SCLC cells, induces changes in cell morphology and suppresses neuroendocrine tumor markers. In addition, valproic acid profoundly inhibits SCLC cell growth. Hubaux *et al* (45) demonstrated that valproic acid improved the efficacy of a second-line regimen (vindesine, doxorubicin and cyclophosphamide) in SCLC cells and mouse models. The advances during the past decades in the genetics and biological pathways driving SCLC have allowed the identification of multiple novel therapeutic strategies. Current studies are underway to explore combinations of immunotherapies, small molecules and chemotherapy with immunotherapy, as well as biomarkers for the selection of immunotherapies.

The present study has certain limitations that may affect its conclusions. First, the conclusions were drawn based on data from public databases rather than actual experiments, indicating that the quality of the data cannot be guaranteed, and that the results may be inaccurate. Furthermore, the propensity of SCLC to metastasize extensively during the early stages of the disease (most commonly to the brain, liver and bone) leads to a 95% mortality rate. However, the M-stage was not considered in the present study, as the M-stage information for all patients in the GSE40275 dataset was recorded as MX. This may affect the accuracy of the present results. Finally, due to a lack of public data on the prognosis of patients with SCLC, the impact of new drugs on survival was not further investigated in the present study.

The present study revealed three novel and powerful diagnostic biomarkers for SCLC based on the chr3 genes CDC25A, FYCO1 and RFTN1. These three genes were significantly associated with pT, stage and sex. In addition, the present study provided suggestions for the development and selection of drugs for clinical treatment based on diagnostic biomarkers. The three aforementioned diagnostic biomarkers may potentially guide the development of novel drugs for SCLC. The present findings may offer novel perspectives for patients with SCLC in future research and clinical applications. However, additional experiments with larger sample sizes are required in order to confirm these conclusions.

Acknowledgements

The authors would like to thank Dr Huai Ning (College of Physical Education, Yunnan Agricultural University, Kunming, Yunnan, China) for providing help with the language.

Funding

This research was funded by the Natural Science Foundation of China (grant no. 81960320), the Priority Union Foundation of Yunnan Provincial Science and Technology Department and Kunming Medical University (grant no. 202001AY070001-199) and the Yunnan Health Training Project of High Level Talents (grant no. D-2019025).

Availability of data and materials

The datasets used and/or analyzed during the current study are available from the corresponding author on reasonable request.

Authors' contributions

HW and JW conceived and designed the study. CM, JZ and YW acquired the data. CM and JZ analyzed and interpreted the data. HW, CM, JZ and YW were involved in the writing, review and revision of the manuscript. HW and JW supervised the study. HW and JW confirm the authenticity of all the raw data. All authors read and approved the final manuscript.

Ethics approval and consent to participate

Not applicable.

Patient consent for publication

Not applicable.

Competing interests

The authors declare that they have no competing interests.

References

1. Semenova EA, Nagel R and Berns A: Origins, genetic landscape, and emerging therapies of small cell lung cancer. Genes Dev 29: 1447-1462, 2015.
2. Bray F, Ferlay J, Soerjomataram I, Siegel RL, Torre LA and Jemal A: Global cancer statistics 2018: GLOBOCAN estimates of incidence and mortality worldwide for 36 cancers in 185 countries. CA cancer J Clin 68: 394-424, 2018.
3. Rudin CM, Brambilla E, Faivre-Finn C and Sage J: Small-cell lung cancer. Nat Rev Dis Primers 7: 3, 2021.
4. Nicholson AG, Chansky K, Crowley J, Beyruti R, Kubota K, Turrisi A, Eberhardt WE, van Meerbeeck J, Rami-Porta R; Staging and Prognostic Factors Committee, *et al*: The international association for the study of lung cancer lung cancer staging project: Proposals for the revision of the clinical and pathologic staging of small cell lung cancer in the forthcoming eighth edition of the TNM classification for lung cancer. J Thorac Oncol 11: 300-311, 2016.
5. Zamay TN, Zamay GS, Kolovskaya OS, Zukov RA, Petrova MM, Gargaun A, Berezovski MV and Kichkailo AS: Current and prospective protein biomarkers of lung cancer. Cancers (Basel) 9: 155, 2017.
6. Liu L, Teng J, Zhang L, Cong P, Yao Y, Sun G, Liu Z, Yu T and Liu M: The combination of the tumor markers suggests the histological diagnosis of lung cancer. Biomed Res Int 2017: 2013989, 2017.
7. Li YL, Roberts ND, Wala JA, Shapira O, Schumacher SE, Kumar K, Khurana E, Waszak S, Korbel JO, Haber JE, *et al*: Patterns of somatic structural variation in human cancer genomes. Nature 578: 112-121, 2020.
8. Zabarovsky ER, Lerman MI and Minna JD: Tumor suppressor genes on chromosome 3p involved in the pathogenesis of lung and other cancers. Oncogene 21: 6915-6935, 2002.
9. Weir BA, Woo MS, Getz G, Perner S, Ding L, Beroukhim R, Lin WM, Province MA, Kraja A, Johnson LA, *et al*: Characterizing the cancer genome in lung adenocarcinoma. Nature 450: 893-898, 2007.
10. Petursdottir TE, Thorsteinsdottir U, Jonasson JG, Moller PH, Huiping C, Bjornsson J, Egilsson V, Imreh S and Ingvarsson S: Interstitial deletions including chromosome 3 common eliminated region 1 (C3CER1) prevail in human solid tumors from 10 different tissues. Genes Chromosomes Cancer 41: 232-242, 2004.
11. Zhou Y, Zhou B, Pache L, Chang M, Khodabakhshi AH, Tanaseichuk O, Benner C and Chanda SK: Metascape provides a biologist-oriented resource for the analysis of systems-level datasets. Nat Commun 10: 1523, 2019.
12. The Gene Ontology Consortium: Expansion of the gene ontology knowledgebase and resources. Nucleic Acids Res 45: D331-D338, 2017.
13. Kanehisa M and Goto S: KEGG: Kyoto encyclopedia of genes and genomes. Nucleic Acids Res 28: 27-30, 2000.
14. Fabregat A, Jupe S, Matthews L, Sidiropoulos K, Gillespie M, Garapati P, Haw R, Jassal B, Korninger F, May B, *et al*: The reactome pathway knowledgebase. Nucleic Acids Res 46: D649-D655, 2018.
15. Schmittgen TD and Livak KJ: Analyzing real-time PCR data by the comparative C(T) method. Nat Protoc 3: 1101-1108, 2008.
16. Sandeep A, Praveen VK, Kartha KK, Karunakaran V and Ajayaghosh A: Supercoiled fibres of self-sorted donor-acceptor stacks: A turn-off/turn-on platform for sensing volatile aromatic compounds. Chem Sci 7: 4460-4467, 2016.
17. Li W, Zhang H, Assaraf YG, Zhao K, Xu XJ, Xie JB, Yang DH and Chen ZS: Overcoming ABC transporter-mediated multidrug resistance: Molecular mechanisms and novel therapeutic drug strategies. Drug Resist Updat 27: 14-29, 2016.
18. Chauncey TR: Drug resistance mechanisms in acute leukemia. Curr Opin Oncol 13: 21-26, 2001.
19. Pérez-Tomás R: Multidrug resistance: Retrospect and prospects in anti-cancer drug treatment. Curr Med Chem 13: 1859-1876, 2006.
20. Zhu MR, Huang Y, Bender ME, Girard L, Kollipara R, Eglenen-Polat B, Naito Y, Savage TK, Huffman KE, Koyama S, *et al*: Evasion of innate immunity contributes to small cell lung cancer progression and metastasis. Cancer Res 81: 1813-1826, 2021.
21. Davis AP, Grondin CJ, Johnson RJ, Sciaky D, Wiegers J, Wiegers TC and Mattingly CJ: Comparative toxicogenomics database (CTD): Update 2021. Nucleic Acids Res 49: D1138-D1143, 2021.
22. Liao Y, Yin GF, Wang X, Zhong P, Fan XM and Huang CL: Identification of candidate genes associated with the pathogenesis of small cell lung cancer via integrated bioinformatics analysis. Oncol Lett 18: 3723-3733, 2019.
23. Shen T and Huang S: The role of Cdc25A in the regulation of cell proliferation and apoptosis. Anticancer Agents Med Chem 12: 631-639, 2012.
24. Sadeghi H, Golalipour M, Yamchi A, Farazmandfar T and Shahbazi M: CDC25A pathway toward tumorigenesis: Molecular targets of CDC25A in cell-cycle regulation. J Cell Biochem 120: 2919-2928, 2019.
25. Ray D, Terao Y, Fuhrken PG, Ma ZQ, DeMayo FJ, Christov K, Heerema NA, Franks R, Tsai SY, Papoutsakis ET and Kiyokawa H: Deregulated CDC25A expression promotes mammary tumorigenesis with genomic instability. Cancer Res 67: 984-991, 2007.
26. Sengupta S, Jana S and Bhattacharyya A: TGF-β-Smad2 dependent activation of CDC 25A plays an important role in cell proliferation through NFAT activation in metastatic breast cancer cells. Cell Signal 26: 240-252, 2014.
27. Brunetto E, Ferrara AM, Rampoldi F, Talarico A, Cin ED, Grassini G, Spagnuolo L, Sassi I, Ferro A, Cuorvo LV, *et al*: CDC25A protein stability represents a previously unrecognized target of HER2 signaling in human breast cancer: Implication for a potential clinical relevance in trastuzumab treatment. Neoplasia 15: 579-590, 2013.
28. Albert H, Santos S, Battaglia E, Brito M, Monteiro C and Bagrel D: Differential expression of CDC25 phosphatases splice variants in human breast cancer cells. Clin Chem Lab Med 49: 1707-1714, 2011.
29. Wang P, Zou F, Zhang X, Li H, Dulak A, Tomko RJ Jr, Lazo JS, Wang Z, Zhang L and Yu J: microRNA-21 negatively regulates Cdc25A and cell cycle progression in colon cancer cells. Cancer Res 69: 8157-8165, 2009.
30. Butz H, Németh K, Czenke D, Likó I, Czirják S, Zivkovic V, Baghy K, Korbonits M, Kovalszky I, Igaz P, *et al*: Systematic investigation of expression of G2/M transition genes reveals CDC25 alteration in nonfunctioning pituitary adenomas. Pathol Oncol Res 23: 633-641, 2017.
31. Rao PC, Begum S, Sahai M and Sriram DS: Coptisine-induced cell cycle arrest at G2/M phase and reactive oxygen species-dependent mitochondria-mediated apoptosis in non-small-cell lung cancer A549 cells. Tumour Biol 39: 1010428317694565, 2017.
32. Olsvik HL, Lamark T, Takagi K, Larsen KB, Evjen G, Øvervatn A, Mizushima T and Johansen T: FYCO1 contains a C-terminally extended, LC3A/B-preferring LC3-interacting Region (LIR) motif required for efficient maturation of autophagosomes during basal autophagy. J Biol Chem 290: 29361-29374, 2015.
33. Dionne LK, Peterman E, Schiel J, Gibieža P, Skeberdis VA, Jimeno A, Wang XJ and Prekeris R: FYCO1 regulates accumulation of post-mitotic midbodies by mediating LC3-dependent midbody degradation. J Cell Sci 130: 4051-4062, 2017.

34. Sillars-Hardebol AH, Carvalho B, de Wit M, Postma C, Delis-van Diemen PM, Mongera S, Ylstra B, van de Wiel MA, Meijer GA and Fijneman RJ: Identification of key genes for carcinogenic pathways associated with colorectal adenoma-to-carcinoma progression. Tumour Biol 31: 89-96, 2010.
35. Eissa S, Matboli M, Awad N and Kotb Y: Identification and validation of a novel autophagy gene expression signature for human bladder cancer patients. Tumor Biology Apr 5, 2017 (Epub ahead of print).
36. Wang J, Qu D, An J, Yuan G and Liu Y: Integrated microarray analysis provided novel insights to the pathogenesis of glaucoma. Mol Med Rep 16: 8735-8746, 2017.
37. Li M, Chen Y, Yao J, Lu S, Guan Y, Xu Y, Liu Q, Sun S, Mi Q, Mei J, *et al*: Genome-wide association study of smoking behavior traits in a Chinese Han population. Front Psychiatry 11: 564239, 2020.
38. Zhao Y, Gao Y, Xu X, Zhou J and Wang H: Multi-omics analysis of genomics, epigenomics and transcriptomics for molecular subtypes and core genes for lung adenocarcinoma. BMC Cancer 21: 257, 2021.
39. Slatore CG, Au DH, Littman AJ, Satia JA and White E: Association of nonsteroidal anti-inflammatory drugs with lung cancer: Results from a large cohort study. Cancer Epidemiol Biomarkers Prev 18: 1203-1207, 2009.
40. Dasari S and Tchounwou PB: Cisplatin in cancer therapy: Molecular mechanisms of action. Eur J Pharmacol 740: 364-378, 2014.
41. Ghosh S: Cisplatin: The first metal based anticancer drug. Bioorg Chem 88: 102925, 2019.
42. Kim JE, Lee SY, Jang M, Choi HK, Kim JH, Chen H, Lim TG, Dong Z and Lee KW: Coumestrol epigenetically suppresses cancer cell proliferation: Coumestrol is a natural haspin kinase inhibitor. Int J Mol Sci 18: 2228, 2017.
43. Que Z, Zhou Z, Luo B, Dong C, Jiang Y, Li H and Tian J: Jingfukang induces anti-cancer activity through oxidative stress-mediated DNA damage in circulating human lung cancer cells. BMC Complement Altern Med 19: 204, 2019.
44. Platta CS, Greenblatt DY, Kunnimalaiyaan M and Chen H: Valproic acid induces Notch1 signaling in small cell lung cancer cells. J Surg Res 148: 31-37, 2008.
45. Hubaux R, Vandermeers F, Cosse JP, Crisanti C, Kapoor V, Albelda SM, Mascaux C, Delvenne P, Hubert P and Willems L: Valproic acid improves second-line regimen of small cell lung carcinoma in preclinical models. ERJ Open Res 1: 00028-2015, 2015.